IN-20
7533
P 49

Advanced Analysis Technique for the Evaluation of Linear Alternators and Linear Motors

Jeffrey C. Holliday
HOLLIDAYLABS
Guysville, Ohio

December 1995

Abstract

A method for the mathematical analysis of linear alternator and linear motor devices and designs is described, and an example of its use is included. The technique seeks to surpass other methods of analysis by including more rigorous treatment of phenomena normally omitted or coarsely approximated such as eddy braking, non-linear material properties, and power losses generated within structures surrounding the device. The technique is broadly applicable to linear alternators and linear motors involving iron yoke structures and moving permanent magnets.

The technique involves the application of Ampérian current equivalents to the modeling of the moving permanent magnet components within a finite element formulation. The resulting steady state and transient mode field solutions can simultaneously account for the moving and static field sources within and around the device.

Technical Background and Motivation for the Advanced Technique

Linear alternators and linear motors have been identified by NASA and others as critical component technologies for Stirling-cycle devices applied to power conversion and thermal management systems. Space and terrestrial uses for these systems include refrigeration, cryocooling, and heat pumping, as well as remote and grid connected power conversion systems fueled by various heat sources (e.g. solar, nuclear, biomass).

These applications typically involve motors or alternators which can be classified as iron yoke, moving permanent magnet devices. Several distinct concepts and design variations of such

devices have been proposed. Evaluation of the relative merits of these designs has been hampered by a lack of broadly applicable techniques for the analysis of different devices within this class. This report presents advanced analysis techniques by which a broad range of differing linear alternator and motor concepts may be thoroughly evaluated. This discussion is presented for the analysis of a typical linear alternator; the technique is used in the same manner to analyze a linear motor.

Figure 1 illustrates a representative linear alternator of the subject class, with basic components identified. Not shown is the surrounding system structure which includes the power piston to which the plunger is typically attached, the power piston cylinder and bearings, the converter pressure vessel, and structural components supporting the stator. A specific linear alternator design following this concept was provided by NASA and is used as a subject for an example analysis in this report. The example alternator has a stationary "stator" component, and a moving "plunger" component, which undergoes a reciprocating motion during operation. The stator consists of the iron yoke and a copper coil for power take-off. The plunger is fitted with permanent magnets.

The linear alternator converts the mechanical energy of the moving plunger into electrical energy. The analysis is concerned with estimating the efficiency of this energy conversion, as well as the apportionment of the various power loss mechanisms. The energy flows involved in a typical linear alternator can be very complex as energy is transduced among the distributed electric and magnetic fields of the system. The nature of these energy flows is dependent on the particular linear alternator design configuration and geometry, and on the design and geometry of the external structures in the neighborhood of the alternator device. The sensitivity to design type has complicated past efforts to

2

use analysis to compare different alternator designs falling within the subject class.

In particular, large magnitude and rapidly varying magnetic fields due to leakage from the intended magnetic circuits of the linear alternator are very configurationally dependent. These fields interact with the structure of the alternator and its environment affecting alternator output power, efficiency, and output voltage. Narrowly-focused design analyses that are configuration specific have been used to estimate performance for some designs, but it may not be accurate to apply these analyses to other members of this class of alternators. This has made even-handed comparison of competing proposed alternator designs or design concepts difficult. A more broadly applicable analysis technique was sought to provide a tool for thorough and accurate comparisons.

Objectives of the Advanced Analysis Technique

The advanced analysis described here was motivated by the need for accurate and detailed methods for alternator analysis in assisting the evaluation of a variety of designs proposed for a particular mission. The objectives for the formulation of the technique were as follows:

1) The analysis should be equally valid in application to any of the alternator design concepts falling in the iron yoke, moving permanent magnet device class;

2) The analysis should not depend on configuration or concept-dependent approximations or empirical formulation;

3) The analysis should treat more rigorously phenomena that are often approximated or ignored in more narrowly-focussed design analysis. These include:

   a) effects due to moving permanent magnet components

b) simultaneous solution of induction effects due to moving permanent magnet and conductor reaction fields
c) non-linear yoke material properties
d) fringing field intensity and distribution
e) non-uniformity of yoke induction fields.

Items a) and b) above are often completely omitted by other analyses, and the accurate treatment of them in this analysis is thought to be unique to this technique. Analysis results involving items c), d), and e) are made more accurate by the treatment of a) and b).

Description of the Advanced Analysis Technique

This advanced analysis technique combines aspects of finite element mathematical formulation methods, which are rapidly developing in the modern computer era, with some useful insight into the nature of magnetization provided by Classical Electromagnetic Physics. Analysts using this technique will need to have access to a finite element analysis package and have some general skill in its use. A general understanding of linear alternators and electromagnetism will also be needed.

Many of the objectives toward thorough evaluation of linear alternator designs can be addressed using finite element computer modeling. Elaborate front ends have been written and marketed for the finite element solvers developed over the past few decades. Several commercially available finite element solver packages have begun to provide capability to address basic electromagnetic field problems. The utility of finite element analysis (FEA) programs for the purpose of this linear alternator

analysis, however, is limited by practical (economic) and fundamental capability concerns.

The commercial FEA package "ANSYS" by Swanson Analysis Systems of Houston, Pennsylvania was chosen for use in the example analysis of this project. ANSYS is one of the better packages in term of capabilities for a variety of electromagnetic field problems. Other FEA packages can also be used with this analysis technique. However, the objectives of this project cannot be met with the FEA tool alone. Rather, FEA provides a framework for the linear alternator analysis technique developed in this project.

Finite element formulation provides an attractive, but limited, tool to remove gross geometrical constraints imposed by narrowly-focused analysis methods. Very small geometrical details of the static structure can be modeled with the finite element formulations. The degree of accuracy of the results and the fineness of detail included in the model can be increased, in general, with increased level of human and computer effort. With attention to balancing the levels of detail and of effort in the formulation, analysts can generate static mathematical FEA models for alternator designs with appropriate and fair consideration to geometrical features and details that differentiate them.

Nonlinear material properties, such as yoke material magnetic permeability, dB/dH, which is dependent on the magnitude of the local magnetic field H, can be included is some FEA formulations. Including nonlinear material properties typically increases the computer time and capacity needed for the field solution phase of the analysis.

5

One key limitation common to all of the FEA packages examined is an inability to adequately model objects in motion directly. This is due to the geometrical fixity required by finite element formulations. Material properties assigned to a particular element representing a fixed location in space cannot be changed during an analysis. This precludes the direct FEA modeling of moving permanent magnet structures and the phenomena associated with the motion of these structures such as output voltage generation and eddy braking power losses. "Gap-type analysis", which allows a limited simulation of a variable gap between components, is not a practical approach for the large displacements of complex components typical in most linear alternator problems.

In order to overcome the analysis barrier represented by the moving magnet material of the linear alternator, this advanced technique involves the construction of a dynamic representation of the moving permanent magnets which allows calculation of the field solution by eliminating reliance on the volume magnetization characterization. The volume magnetization, or magnetic moment density, is a material property which would require assignment to elements within a finite element formulation and would not allow motion of those elements.

Instead of a direct representation of the permanent magnets as a volume of material with distribution of magnetic moment density, the permanent magnet structures are here represented as a collection of current densities flowing in free space within or on the surface of the magnet volume. These currents are imposed on the finite element formulation as nodal or elemental current loading and, as such, can be changed over time to simulate the motion of the magnets. This is in contrast to direct material property modeling of the magnets.

These current densities are chosen to provide a model mathematically equivalent to the model using direct magnetized material representation. Such a model is called an Ampérian current equivalent, Ampére having used the analogy during the nineteenth century. The goal of the analysis model representation of the physical alternator system is to provide the framework of equations to calculate the magnetic field distribution due to the physical system. This information is contained in the solution to the magnetic vector potential function A. Two representations that produce the same magnetic vector potential are equivalent.

The equivalence of the Ampérian current representation is assured provided the current distribution at any point in space is chosen to be the vector curl of the magnetization distribution it is to represent.

Eq. 1 $$J = \triangledown \times M$$

where: J is the equivalent current density distribution,

M is the volume magnetization of the magnet,

$\triangledown \times$ is the vector curl operator

and both J and M are vector functions of space.

The general equivalence of the Ampérian representation can be demonstrated by the exercise of proving the mathematical identity of the closed form vector potential solutions obtained through the use of the following two representations for an arbitrary magnetized volume (Lorrain and Corson, <u>Electromagnetic Fields and Waves</u>, page 386, chapter 9, copyright 1970, W. H. Freeman and Company, San Francisco).

1) In closed form, the magnetic vector potential distribution, A, in space due to an arbitrary volume, τ, of material with a magnetic moment density distribution, M, is, for points outside of the volume:

$$A = \frac{\mu_0}{4\pi} \int \frac{M \times r}{R^2} \, d\tau$$

where R is the vector from the location of the differential volume, $d\tau$, to the point where the potential is calculated, r is the unit length vector in the direction of R, μ_0 is the permeability of free space and the integral is over the volume τ.

2) In closed form, the magnetic vector potential distribution, A, in space due to the distribution of Ampérian current equivalents, J, on and within the same arbitrary volume τ, is, for points outside of the volume:

$$A = \frac{\mu_0}{4\pi} \int \frac{J}{R} \, d\tau$$

3) Mathematical identity of these two expressions is valid if the condition of equation 1 is applied. A similar exercise for points of space inside of the arbitrary volume can be conducted as well (see Lorrain and Corson.)

The equivalent current distributions for each magnet of the alternator are summed to provide a total distribution of equivalent currents for this representation. This current distribution will shift in space as the movement of the physical magnets is simulated. The equivalent current at each location in space within the swept volume of the magnet assembly will have a time dependency relating to the motion of the magnets. The

description of the current at a point over one period of the plunger motion is called the equivalent current profile for that point.

To accommodate the discrete nature of the finite element formulation, both the spacial and the temporal descriptions of the equivalent current distribution must be discretized and loaded into the finite element formulation for solution as a time-transient field problem. This current loading must be applied to elements or nodes in accordance with the capability of the FEA package and the type of current density involved. Ampérian current densities on a surface may best be modeled using nodal loading. Volume current densities may be better applied as elemental loading.

The solution for the magnetic vector potential over the time of interest is now computed using the FEA code. For analysis directed toward steady state operation of the alternator system, the solution over the period via the time transient calculation is repeated until a condition of periodicity is met.

Once this time history of the field solution over space is obtained, the analysis problem becomes straightforward. Results based on the time dependant field solution can be derived to satisfy particular objectives of the analysis effort. For example, gross power loss in structures, heat generation distribution in these structures, and the spacial mapping of loss sensitivity of the design can be calculated.

<u>Step by Step Summary for the Application of the Technique</u>

a)   Decide what is important in the problem and what should be included in the model. Create a solid model of the

alternator components. Force axisymmetry if computer system
is taxed. Remotely locate an infinite boundary to
accommodate leakage fields. This first step is critical as
the accuracy and economy of the remainder of the analysis
depend on these selections.

b)   Model the volume swept by the plunger magnets with a mesh of
      small uniform elements. An element width much less than the
      plunger displacement amplitude should be used. In
      developing this mesh, consideration should be given to the
      plunger position waveform and the requirements of step e)
      below. This mesh should include element nodes coincident
      with the location of the permanent magnetization gradients,
      particularly at the edges of the permanent magnet
      structures, during each of the time instants chosen in step
      e) below.

c)   Develop a satisfactory element mesh distribution for all
      areas outside of the swept volume. In each analysis case, a
      balance must be struck between accuracy targets and the
      economy of the analysis. The mesh should be finer in areas
      experiencing large changes with time in the magnetic field
      vector or large field gradients over space. Larger element
      sizes are acceptable near the infinite boundary and in other
      areas of low field activity. The air in narrow gap regions
      such as that between the plunger and yoke should be modelled
      using at least two element widths across the gap.

d)   Make appropriate material property assignments such as
      electric resistivity and magnetic permeability for the
      elements comprising the components of the alternator.
      Material properties should be defined to a level of detail
      consistent with the analysis objectives and predicted
      conditions experienced by the material. Nonlinearity,

temperature dependance and anisotropy in the characterization of the material properties can be included. Direct modeling of the permanent magnet requires that material property tables to describe the permanent magnet materials be developed. Permanent magnet material property information is also used in the formulation of the Ampérian current equivalent.

e)   From the plunger position waveform, select particular positions and tabulate the associated time instants in the period. Calculate the time increments between successive instants. The selected set of positions and instants need not be spatially or temporally uniform. However, it is useful to have generated the mesh of step c) with foresight to this task. Nodes should be provided at locations with large magnetization gradients, such as at the magnet edges, at each of the chosen instants.

f)   From the set of plunger positions, select points of interest for the verification of the equivalent current model. Conduct static field solutions at these particular plunger positions with the permanent magnet material properties assigned to the elements coincident with the magnet locations at that instant. Other elements in the swept volume are assigned the material properties of air or another default material, such as that from which the balance of the plunger is composed.

g)   Conduct static field solutions for these particular positions using the equivalent current representation. All of the swept volume elements are assigned the properties of air or other default material. Specific nodes representing locations of the Ampérian current equivalents are turned on by assigning those currents to those nodes.

h)   Comparison of the results of the direct modeling of the
     permanent magnet material of step f) to the results of the
     equivalent current model (step g) can be used to guide
     modification of the node locations and current assignments
     to obtain the level of agreement required of the analysis.
     These two methods should produce solutions for the static
     field that are equivalent to the degree allowed by the level
     of detail involved in the model. This comparison is
     particularly useful if severe or non-uniform demagnetization
     of the permanent magnets in the device confound the
     discretization of the Ampérian current equivalents.
     Comparison at several points in the cycle and interpretation
     of the results should identify this condition. In such
     cases, the Ampérian current equivalent will involve
     significant volume current densities as well as surface
     currents. A more complex set of node and/or element
     loadings will be needed to model this current distribution
     adequately. Surface current densities are typically the
     only loadings required in more straightforward problems such
     as the example in the next section.

i)   Create tables of the Ampérian current equivalent profiles
     for the nodes and elements having non-zero equivalent
     currents at any of the time instants of the selected set.
     The equivalent current profiles should include the value of
     the current to be assigned during each of the time instants
     that make up the period. Similarly, node and element
     current loadings arising from real currents in the system,
     such as that of the power takeoff, should be tabulated to
     facilitate impressing them into the time transient analysis
     to be performed in the next steps.

j) Set up a finite element time transient solution over the full period including time steps of appropriate size to match the time instants chosen. Node and element current loadings should correspond to the Ampérian current equivalents and real current profiles for each instant. Additional time steps for current load ramping or intermediate time approximations can be used as needed for numerical stability and accuracy concerns.

k) Execute the transient solution over the first period. Initial conditions must be specified. If no estimate is available for the periodic steady state values expected for the beginning instant of the period, the static field solution corresponding to the initial plunger position may be used.

l) Execute successive transient solutions over the period using the results of the previous period as initial conditions for the new period. Compare results for a particular time instant or instants to those of the previous period. Once a satisfactory degree of repetition has been obtained, the results of the final period may be used for postprocessing in the next step. Until that condition is met, the foregoing results are considered transient in that the alternator system model has not settled into a periodic steady state. Unless there is specific interest in this transient response, this data may be erased in the interest of conserving computer storage capacity.

m) Solution results from each of the chosen time instants of the final period are now taken to postprocessing to calculate analysis results of interest to the particular study. This data represents the periodic steady state response of the alternator system. Calculable results that

will be useful in design evaluation include:

- Eddy current losses, including eddy braking which involves the transduction of mechanical power into heat and a slowing of the plunger resulting from eddy currents associated with the motion of the magnets as distinguished from eddy currents arising from changes in the power take-off current.

- Mapping of the loss sensitivity of the system structural design, derived from the time derivative of local field intensity at locations surrounding the alternator proper. This can be used to evaluate various designs and may influence selection of the device configuration, location and material of the necessary surrounding structure, and possibly selection of other component configurations in the vicinity of the device (e.g. bearings).

- Power loss breakdown for the components of the device and its surrounding structure.

- Operating performance aspects such as output voltage, power, and impedance. Limitations and nominal ratings can be explored.

Example Application of the Advanced Analysis Technique

For the purpose of an example application of the advanced analysis technique, a representative linear alternator design was provided by NASA LeRC. This conceptual design was generated by Mechanical Technology Inc. (MTI) in a DOE-funded project targeting terrestrial solar dynamic energy conversion systems;

NASA LeRC provided technical management for this project. The system concept investigated involved a linear alternator directly coupled with a Stirling heat engine. This conceptual design is described in NASA CR-180890, January 1988, "Conceptual Design of an Advanced Stirling Conversion System for Terrestrial Power Generation."

The example application follows the step-by-step summary discussed in the previous section. The labeled steps in this example refer to the steps of the step-by-step summary.

Step a):

The FEA solid model approximating the linear alternator design for this example analysis is shown in figure 2. The model is cylindrically axisymmetric, which allows a two-dimensional finite element formulation to be used for the analysis. Use of this approximate model results in significant savings in the amounts of computer capacity and computer time required to complete the analysis. This restriction of symmetry precludes the evaluation of azimuthal magnetic field effects, which were felt to be relatively unimportant for this illustrative example. This exclusion is due to this particular choice of symmetry restriction and is not an inherent limitation of the advanced analysis technique in general. Azimuthal magnetic field effects can be analyzed using solid models that include important feature details in all three dimensions.

In the example alternator, two components form a slotted iron yoke which surrounds a single power takeoff winding. All of these structures remain static during the alternator operation. The "external structure" identified in figure 2 is included to represent the converter pressure vessel, power piston cylinder, and other structures in the immediate environment of the alternator. The terms "external structure" and "surrounding

structure" are used interchangeably in this report.

Figure 2 indicates the nominal plunger end-of-stroke position by the location of the three permanent magnets which are all a part of the plunger in the physical alternator. The additional volume swept by any magnet in the course of a machine cycle is identified by shaded areas as labeled. The magnets form three rings concentric with the machine axis and arranged in a closely-separated stack. Each magnet ring has a radially magnetized vector direction, and adjacent rings have opposite sense. The poles of the magnets are on the inside and outside cylindrical faces of the rings. The rest of the plunger structure is treated as nonconductive nonmagnetic material and, therefore, is modeled as air.

In anticipation of the requirement for reasonable field solution results in the regions outside the alternator proper, the solid model includes a specified volume of air surrounded by an "infinite boundary". This model will include direct elemental representation of the volume within the boundary and the imposition of a zero magnetic potential condition at the boundary. The boundary is located at a distance from the center of the yoke cross section of at least 1.5 times the magnet ring radius. This should provide for a good examination of the fringing magnetic fields and their consequences. After the analysis is completed, the magnetic field gradient near the infinite boundary should be checked to see if the location of the boundary appears satisfactory.

Steps b-c):

Features of the finite element mesh developed for use in this example alternator analysis are illustrated in figures 3 and 4. Element shapes that are considered robust, i.e. not prone to certain errors such as averaging or interpolation errors, are

16

used throughout. A very course mesh is used near the infinite
boundary, which is an area expected to have zero or near-zero
magnetic fields. A much finer mesh is used where the field
solution is expected to be most interesting or significant. The
very thin cylindrical air gap between the yoke and magnet swept
volume is modeled with a mesh several elements thick; the mesh
for this air gap is shown in figure 3, but is finer than the
printing resolution. The mesh of the support structure is
blanked out in figure 3 to highlight the location of this
component. The mesh for this component involves a
straightforward transition of element sizes to match the mesh of
the neighboring regions which are shown in the figure.

The mesh in the transition areas between these very small
dimensioned elements and larger mean element sizes was refined to
reduce the number of elements with due consideration to accuracy
concerns. This mesh refinement reduces the overall computer
capacity and time involved in the field solution phase of the
analysis and contributes to the overall economy of the effort.

The volume swept by the permanent magnet rings is meshed
with an array of small rectangular elements as shown in figure 4.
Note that these elements are actually all uniform although they
do not appear to be so in the figure. This regular pattern
facilitates the generation and assignment of the equivalent
current distribution profiles later in the analysis.

The breakout of elements by structure for this example is:
1660 elements -- Magnet swept volume
 854 elements -- Yoke material
 170 elements -- Power takeoff conductor
 267 elements -- External structure
 790 elements -- Air gap just outside of magnet swept volume
1754 elements -- Other air regions
5495 elements --   Total model

Step d):

Material property descriptions were chosen and assigned to the elements of the model. A steady state operating temperature of 60 Celsius was assumed, and any dependance of material properties for temperature variations around steady state was not included in this example. Such temperature dependance of material properties can be included in this technique and may be particularly appropriate in applications exploring thermal management or cooling of the device. These cases require the use of coupled-field (thermal and electromagnetic) FEA solutions and will likely require iterative solution steps.

The external structure identified in figure 2 is a representative single component composed of a non-magnetic stainless steel. Elements modelling this material were given a linear electrical resistivity and a linear relative permeability equal to that of type 316 stainless steel.

The example alternator design calls for non-oriented M-19 silicon-iron (Si-Fe) electrical steel for the yoke components. This material was assigned a nonlinear, isotropic characterization for magnetic permeance. This characterization is represented in the curve of B vs H for the material plotted in figure 5. This representation closely follows a manufacturer's property character data plot in the low field linear region and in the very non-linear "knee" region. The large field region exhibits the saturation character with permeabilities approaching that of air; the curve for this region had to be extrapolated due to lack of manufacturer's data. The representation in the large field region can affect numerical stability of the FEA solution, and a slight overestimate of the material response at large fields (as recommended in the ANSYS manual) can be used to obtain a stable FEA solution that can highlight saturating regions for

further characterization or design refinement as needed. This slight overestimate was included in the large field region of the curve.

The power takeoff winding was modeled using the electrical conductivity of copper at the specified temperature (60 C), and unity relative magnetic permeability.

Material properties for the direct representation of the permanent magnets were used for the static solutions of step f). Neodymium-Iron-Boron magnet material grade NeIGT 30 H was specified, and demagnetization data from the manufacturer, IG Technologies, was used for the characterization. These magnet properties were also used in the formulation of the Ampérian current equivalent.

Step e):
The motion of the example alternator plunger in the operating Stirling-cycle converter is a sixty hertz oscillation with an 18 millimeter amplitude. A trace of this plunger position for one period is shown in figure 6. A set of 36 points representing specific instants were chosen for the discretized representation for this motion. These points are marked on the curve of figure 6. The period is thus divided into 36 time-intervals or time-steps.

Further subdivision of each of these time-steps into two substeps will be carried out automatically during the FEA solution during steps k) and l). The ANSYS program will "ramp" applied loads by interpolating any loads that change during the time-step, and will calculate solutions for each of the 72 substeps. Only those solutions corresponding with the endpoints of each time-step were saved. Gradually ramping loads over several substeps within a time-step helps to satisfy time

transient integration requirements for convergence to an accurate
FEA solution, especially when nonlinear material properties are
involved.

The chosen points or steps are uniformly spaced in terms of
the plunger position, being at intervals of 2.0 mm. The mesh of
the swept volume was generated with this spacing in mind. Nodes
have been provided at locations corresponding to the physical
magnet edges at all the chosen time/plunger position points.

The chosen points or steps are not uniformly spaced
temporally. The time interval between successive points is
larger near the stroke-ends where the plunger velocity is
smallest. The time interval is smallest near the midstroke where
the plunger velocity is greatest.

Steps f-h):
        The Ampérian current equivalent representation for a
permanent magnet ring similar to those of the example alternator
is shown in figure 7. The direct representation for this magnet
as a volume of magnetized material is shown in figure 8. The
example alternator magnet rings are composed of rare-earth grade
hard magnetic material (Neodymium-Iron-Boron) with essentially
uniform internal magnetization. As shown in figure 7, the
equivalent current distribution for this uniform internal
magnetization is zero current within the bulk of the magnet
volume and a finite surface current density on only the axial end
surfaces of the magnet volume. This character follows directly
from the vector curl of the magnetization, which is discontinuous
at the magnet surface and uniform elsewhere (see eq. 1). The
curl of a function is zero where it is uniform, as all of the
partial differentials of its components are zero. On the
cylindrical surfaces (the magnet poles), the only non-zero
partial differential is the radial component with respect to the

radial direction, which is not involved in the vector curl. On the axial end surfaces, the partial differential of the radial component with respect to the axial direction is non-zero, and equal to the radial magnetization, in this case; this results in the non-zero azimuthal component for the vector curl shown in figure 7.

For the example alternator, the magnet rings are modeled with uniform radial magnetization of 716,000 Amps per meter (9000 Oe), consistent with the manufacturer data derated for the 60 Celsius operating temperature. Each axial end of each magnet has a uniform current density of 716,000 Amps per meter and a width of 10 mm. Thus a total current of 7,160 Amps flows on each axial end surface; the direction of this current is in accordance with the polarity of the magnet ring and the relative location of the end surface. Nodal current loading was used in the finite element formulation of this Ampérian current equivalent for each of the three permanent magnet rings in the example device. A row of 11 nodes (see figure 4) is coincident with each magnet edge at the chosen instants. The two nodes at either end of this row (coincident with the magnet "corners") are assigned a smaller current loading than that assigned to the remainder of the nodes to account for how ANSYS distributes the current loading along the line of nodes. The nodal loading for these other nine nodes was uniform across the edge and was set at 716 Amps for each node. The corner nodes were assigned 358 Amps each. This loading models a 7,160 Amp current sheet extending between these eleven nodes. Nodes not coincident with a magnet edge at an instant were assigned zero current loading.

This Ampérian current equivalent representation provides field solution results exhibiting very good agreement with those of direct modeling of the permanent magnet (see following discussion). This was confirmed by producing and comparing

static field solutions for a severe-case plunger position using
the same FEA mesh for both the direct permanent magnet modeling
and the Ampérian current equivalent model.

The degree of agreement between the solution results is
dependent on 1) the quality of the finite element mesh common to
both analyses, and 2) the quality of the discretized
representation for the Ampérian current equivalent. A greater
degree of agreement can be expected from a more refined Ampérian
current representation. For instance, in this example, the nodal
current loading could be further refined by adjusting the
impressed load according to the radial position of the nodes
(node locations vary over plus or minus 5 mm around a median of
135.5mm)

Figure 9 is a mapping of the percent difference in the
magnetic field solution in the yoke determined by using the
Ampérian current equivalent technique relative to the direct
modeling technique for the plunger end-of-stroke position.
Differences between the two techniques should be near their
largest values for this plunger position. A value of 0.01 in
this figure indicates that the induction field results differ by
less than 1%. Almost all of the yoke is seen to have results
that are in agreement within less than one-half of one percent.

Figure 10 is a plot of the magnetic field solution in the
yoke, represented by flux-lines, for the plunger end-of-stroke
position. This plot reveals a few small regions of high field
gradient where the field diverges and then leaks out of the yoke.
Greater solution variance and sensitivity to mesh character and
other factors can be expected in such regions. The solution
differences in these small high-gradient regions are seen (figure
9) to range from 1% to 5%. Other model areas that may be
particularly sensitive to solution variance include regions where

the discrete nature of the mesh or loading is large relative to the geometry or field gradients (e.g. within one element width of the magnet edge.) This is typical of all analyses that rely on the FEA discretized characterization of physical systems.

In this example, the solution differences of greatest concern were in the yoke; all other areas had differences of less than one-half of one percent of the maximum yoke field, except for very small regions near the magnet corners which had differences approaching one to two percent. Overall, the differences (including those in the yoke) are felt to be reasonable and are not expected to have a significant impact on the final solution.

Step i):
As discussed in step e) and shown in figure 6, the period of the plunger motion was divided into 36 steps. The timespans for these steps were computed. The Ampérian current distributions at each of these instants were generated as previously described. The equivalent current profiles were loaded for each node within the magnet swept volume. Figure 11 is a plot of the load profile for one representative node in the magnet swept volume. This node's load is seen to be "off" (zero) except at times when its location is coincident with one of the magnet edges. The direction (sign) of the applied current load depends on which one of the magnet edges is involved.

Elemental loading was used for the prescribed load current in the winding (the real power takeoff). The power takeoff current was assumed to be sinusoidal and have a power factor of 1.0 (i.e. no net reactance). This current waveform was discretized to allow the loading at the chosen instants. The phasing of this power takeoff current results in an element current loading of zero when the plunger is at the stroke end,

and a maximum when the plunger is at the midstroke. Figure 12
illustrates the discretization used to load the real currents
into the elements modeling the winding. Currents up to 125 Arms,
corresponding to the design's nominal full power output rating of
30kWe, were explored.

Steps j-l):

An initial set of conditions for the magnetic vector
potential throughout the model was chosen. The position of the
plunger at the beginning of the representative period is at the
endstroke, and the power takeoff current is zero at that time.
The magnetic vector potential solution resulting from a static
analysis using the Ampérian current equivalents for that position
and a zero power takeoff current was used. The magnetic vector
potential solution as a function of time was then sought using
the ANSYS time-transient mode and 36 time-steps (each with two
intermediate sub-steps for load ramping – in parlance of ANSYS,
this means one additional solution will be calculated during each
time-step) over the period for a total of five periods. This
solution phase was carried out using the node and element current
loading profiles generated in step i).

The set of results for the last full period of this solution
phase was saved for postprocessing as the "periodic steady-
state". In order to verify that a satisfactory level of periodic
repetition had been obtained, a variety of specific solution
results were examined and recorded as the solution progressed.
Both "instantaneous" and cycle integral results were charted.

Figure 13 is a table of one of the solution results that was
so tracked, expressed in terms of percent change from the result
that was recorded one period earlier. A value of 0.00 indicates
complete agreement (8 significant figures) with the previous
period. The tracked solution result of figure 13 is the rate of

power loss (average for the time-step interval) within the stainless steel structure that surrounds the linear alternator for the 125 Arms takeoff case; this was calculated to at least nine significant figures at each step. The variance of the result is seen to settle down very quickly from the initial perturbation. The waveform over the cycle of this power loss is shown in figure 14 - see step m). For many systems, the solution phase can be restricted to only three or so periods and will still yield an accurate representation of the periodic steady state. This example problem required about a 22 hour solution time on a 100 Hz 80486 computer for five full cycles.

Step m):

The set of results computed for the last full period of the solution phase was saved for postprocessing as the "periodic steady-state". One such set was recorded for each power takeoff case examined (open circuit and nominal full power output at 125 Arms). A variety of results of interest can be distilled from these periodic steady-state field descriptions, providing device performance predictions, support system requirements (e.g. heat rejection needs) and insight useful for design revision or improvements of the device.

The rate of power loss in the surrounding structure of the alternator (the result that was tracked during the solution phase - see figure 13) for the 125 Arms output case is shown to vary over the cycle in figure 14. The dashed line indicates the cycle averaged power loss in this entire component. This power loss is manifested by heat generation via eddy currents in the stainless steel structure. The distribution of this heat generation (power loss) throughout the surrounding structure is illustrated by figure 15 which is a plot of the instantaneous power density for a particular time in the cycle (again for the 125 Arms output case). The particular instant shown is the end of the fifth step

from the period start. (For plunger position, see figure 6; this is also the time instant involved in figures 16 and 17.) The integral of this power density over the volume of the surrounding structure is the total power loss in the surrounding structure at that instant.

Results such as these are useful in efforts to identify locations prone to structural power losses for design refinement or evaluation. In this example, most of the power loss arises in the area representing the inner piston cylinder. Such a condition may impact bearing operation or require cooling.

The loss in the surrounding structure for the full output power simulation is 367.6 W. Note that this loss represents more than one percentage point in alternator efficiency for this nominal 30-kW output alternator. During open circuit (i.e zero power take-off current) operation, the power loss in the surrounding structure components is strictly due to eddy braking. The component loss at this open circuit operating condition was calculated at 20.5 W.

Fringing fields and the attendant space sensitivity to power losses in external structures can be mapped as in figure 16. In this figure, each flux line represents 2% of the total flux present in the model at the instant at the end of the fifth step for the 125 Arms output case. This kind of information is particularly useful to guide the design of supporting or peripheral structures in the neighborhood of the alternator device. It can also be used to more broadly evaluate alternator design concepts or designs when details regarding surrounding objects are not well known or defined.

The magnitude of the power loss in the surrounding structure at the full output power is due in part to the saturation

phenomenon in the yoke components, which can be better understood by examining information like that of figure 17. Figure 17 is a plot of the local instantaneous permeability of the yoke material (normalized to the low-field linear permeability for this material) at the end of the fifth step in the full output power case (125 Arms). The low permeabilities indicated by shading in much of the yoke are an indication of hard saturation of this material. Greater leaked fields (figure 16) are one result of this condition. Such leaked fields are ultimately responsible for the power losses in the surrounding structure.

The information of figures 15-17 was plotted for every step (2 mm intervals of the plunger motion, 36 steps total) of the 125 Arms full output power case. This type of information can be integrated to determine total structural power loss as shown in figure 14 and can also be examined to locate design problem areas and evaluate their behavior over the course of the cycle.

The accurate and detailed magnetic field solution over space and time is the crucial result of this analysis technique. The information provided in this field solution is the basis for further postprocessing for calculation of particular quantities of interest to the analysis at hand. The details of such field solution postprocessing will depend on the specific analysis goals and can be carried out in the same manner as the analyst normally would calculate such results from any magnetic field solution and history. In the example alternator analysis, emphasis was placed on using the field solutions to examine power loss phenomena in the surrounding structure. Other aspects of alternator performance can be calculated or derived from the field solution and history. Output power and overall efficiency of the device can be determined by calculating the generated voltage from the flux linkage and properly accounting for power losses in the winding, yoke, magnets and surrounding structure.

This advanced analysis technique can provide a more accurate estimation of such operating characteristics because it simultaneously involves both the moving permanent magnet and the conductor reaction field sources in the calculation.

Phenomena Not Illustrated by the Example Analysis.

The example analysis here presented does not illustrate rigorous treatment of the effects associated with:
- Azimuthal magnetic fields
- Non-isotropic material properties
- Movement of yoke or conductor material components.

These phenomena were excluded in consideration of the practical limitations of available computer power and time and due to the limitations of available finite element solvers. Of the three areas noted, the first two can be included in a straightforward way in this advanced analysis technique. Accommodating the third area would require some significant changes to the analysis approach and may not favor the use of finite element formulation.

Azimuthal magnetic fields were excluded as a consequence of the choice to restrict the mathematical model to cylindrically symmetric geometry. This restriction to two dimensions substantially reduces the required time and computer capacity, but it precludes any non-zero components of the magnetic field vector in the azimuthal direction. Typically, the most salient features differentiating alternator designs, such as the number or arrangement of permanent magnet rings, can be adequately explored without regard to the azimuthal details. In such cases, the economy offered by the two-dimensional model may counterbalance the loss of some fine detail information.

Non-isotropic yoke materials used in some alternator and motor designs have material properties that are directionally dependent and can confound finite element formulation. Some FEA packages allow the direct definition of nonisotropic material properties, but this treatment is not available in most FEA packages. Short of using the more powerful FEA packages for direct formulation, the analyst can include a representation of non-isotropic materials by assigning a range of material types to the yoke elements according to the direction of the expected field result for each element relative to the material "grain", or preferred field orientation. Each region of the yoke can be assigned a different isotropic permeability curve approximating the natural response of the material to fields with the expected magnetic field direction for that region relative to the orientation of the grain of the anisotropy. The analysis is then conducted using this piecewise description of the solid model.

The movement of yoke or conductor materials (in addition to the moving magnets) during operation of the motor or alternator device can not be analyzed directly in this technique. The methods used to represent the motion of the permanent magnet materials in the device via Ampérian current equivalents are not applicable to these other materials. Some estimate of the external magnetic fields that these components might experience during their travel, and the resultant power losses, can be made with the aid of the existing technique.

Concluding Remarks

The analysis technique presented here can provide a basis for thorough and accurate comparisons of competing linear alternator or linear motor designs or design concepts proposed

29

for particular missions of interest. The technique can also be used for indepth analysis of a particular design, to guide design refinement.   The technique is applicable to any linear alternator or linear motor design concept of the iron yoke, moving permanent magnet class.

The analysis provides special treatment of moving permanent magnet components using Ampérian current equivalents within a finite element formulation. This allows the simultaneous solution of the magnetic vector potential due to both the moving permanent magnets and conductor reaction fields. Rigorous treatment of eddy braking, yoke saturation, and structural power loss calculations can be made using the technique.

A next step would be to compare test results from existing linear alternators or linear motors with predictions from this technique to allow validation and modification as required. This would be particularly useful to do with existing hardware that could be accurately modeled or possibly with hardware that could be specifically built for verification purposes to be easy to model.

PLUNGER

AZIMUTHAL DIRECTION

STATOR

AXIS OF MOTION AND DEVICE CENTERLINE
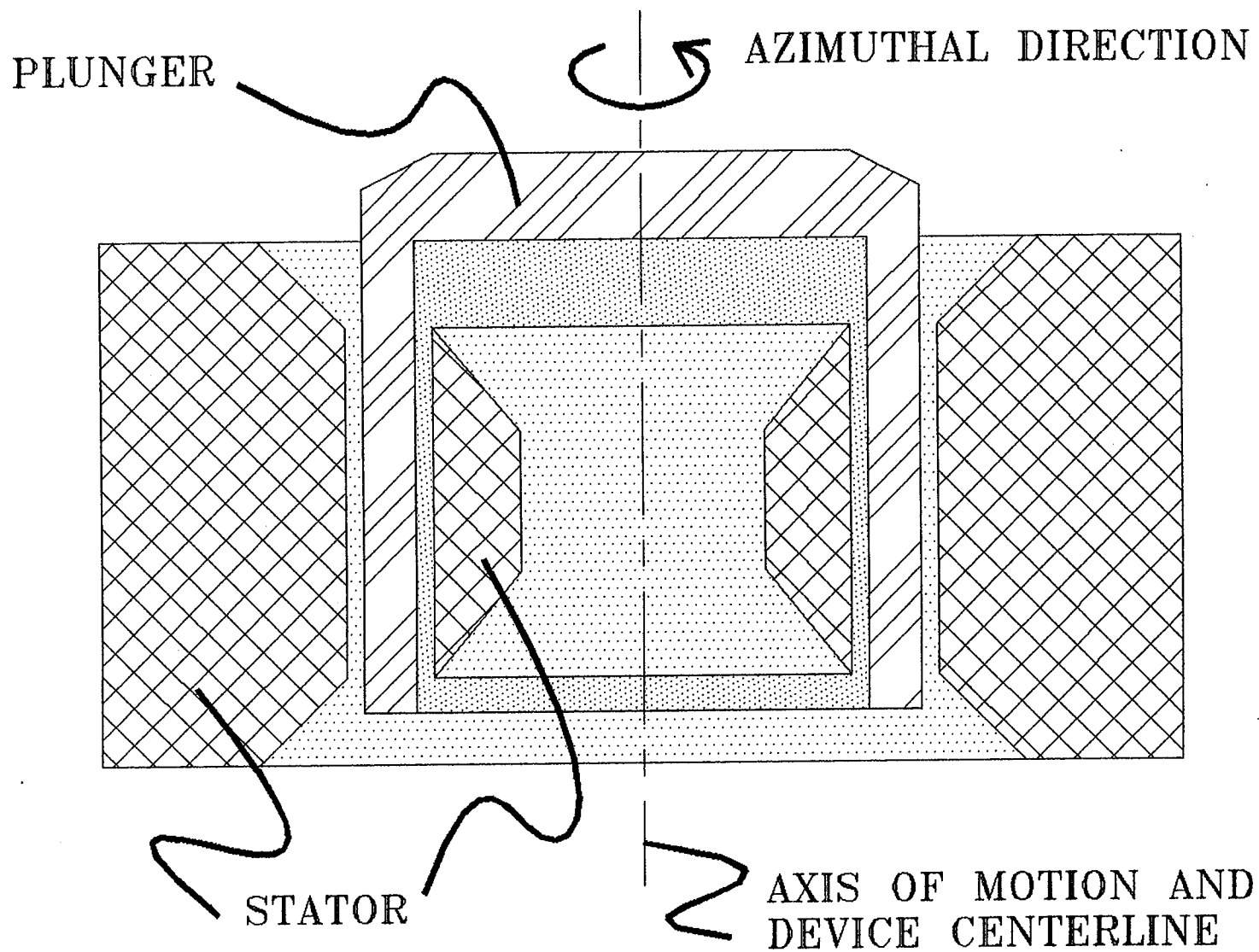
FIGURE 1 — TYPICAL LINEAR ALTERNATOR DEVICE

AXIS OF SYMMETRY

EXTERNAL
STRUCTURE

MAGNETS

YOKE

WINDING

YOKE

AIR

MAGNETS

INFINITE
BOUNDARY

ADDITIONAL
SWEPT VOLUME
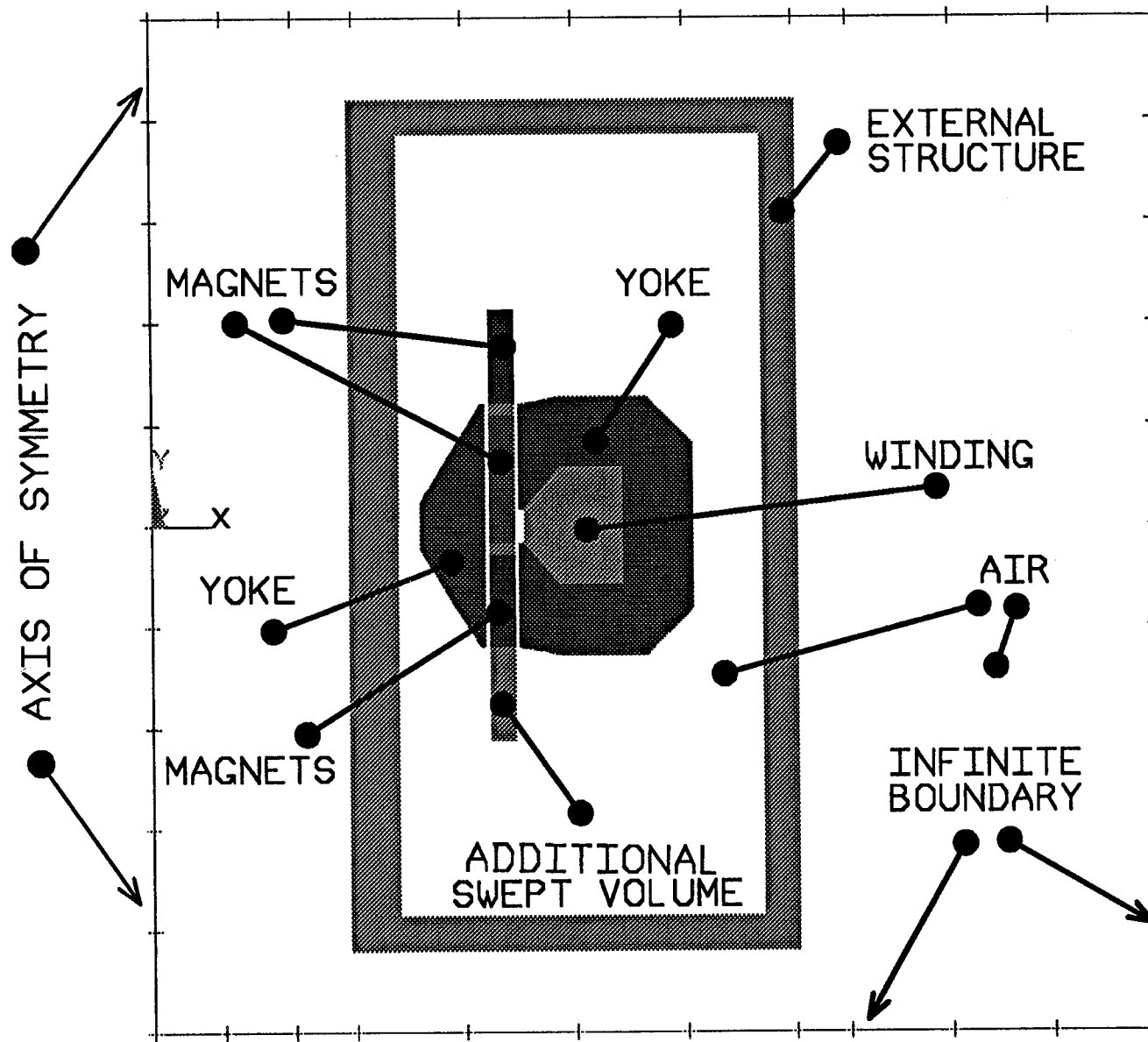
Figure 2 - Solid Model of Example Linear Alternator
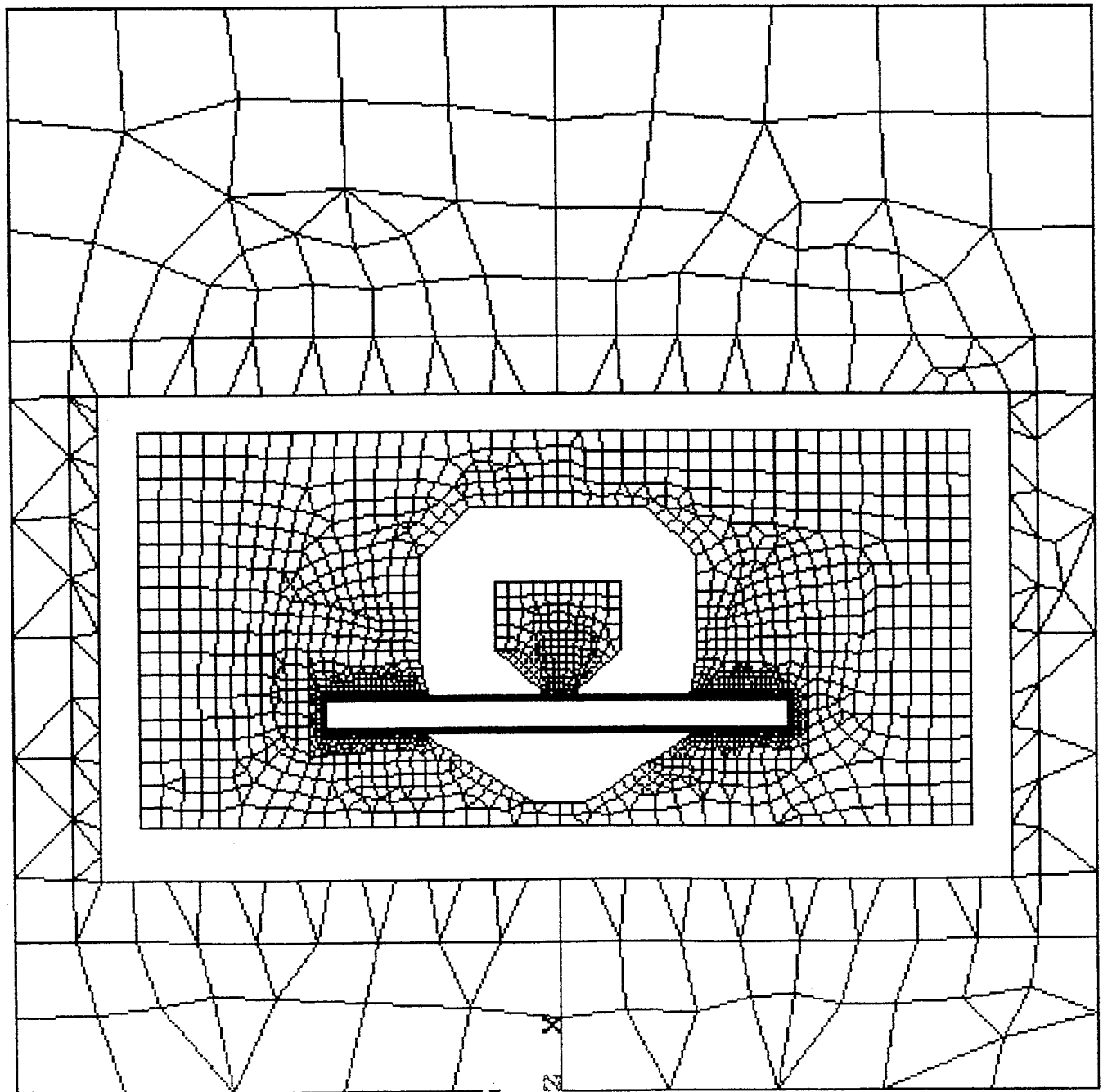
Figure 3 - ELEMENT MESH for AIR REGIONS and POWER TAKEOFF CONDUCTOR

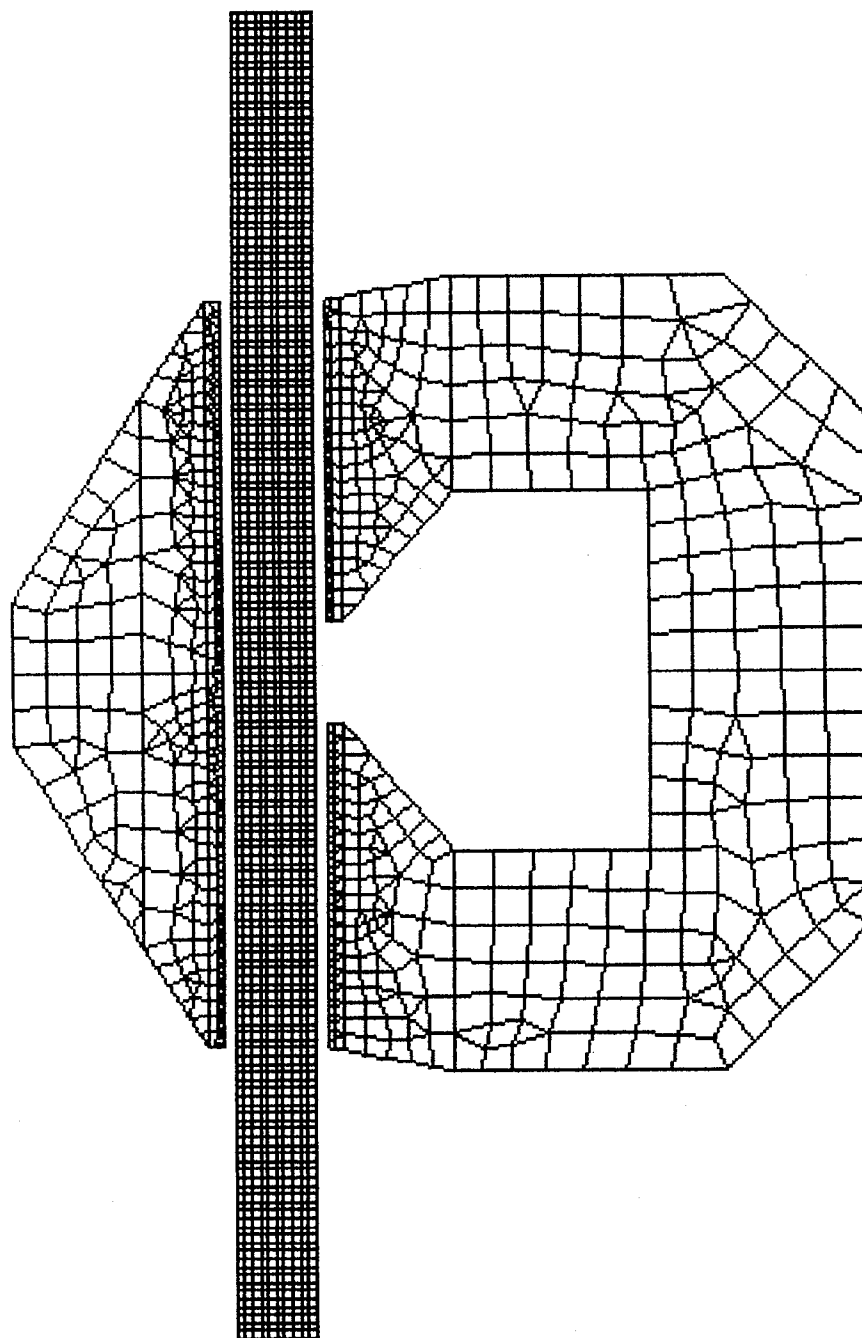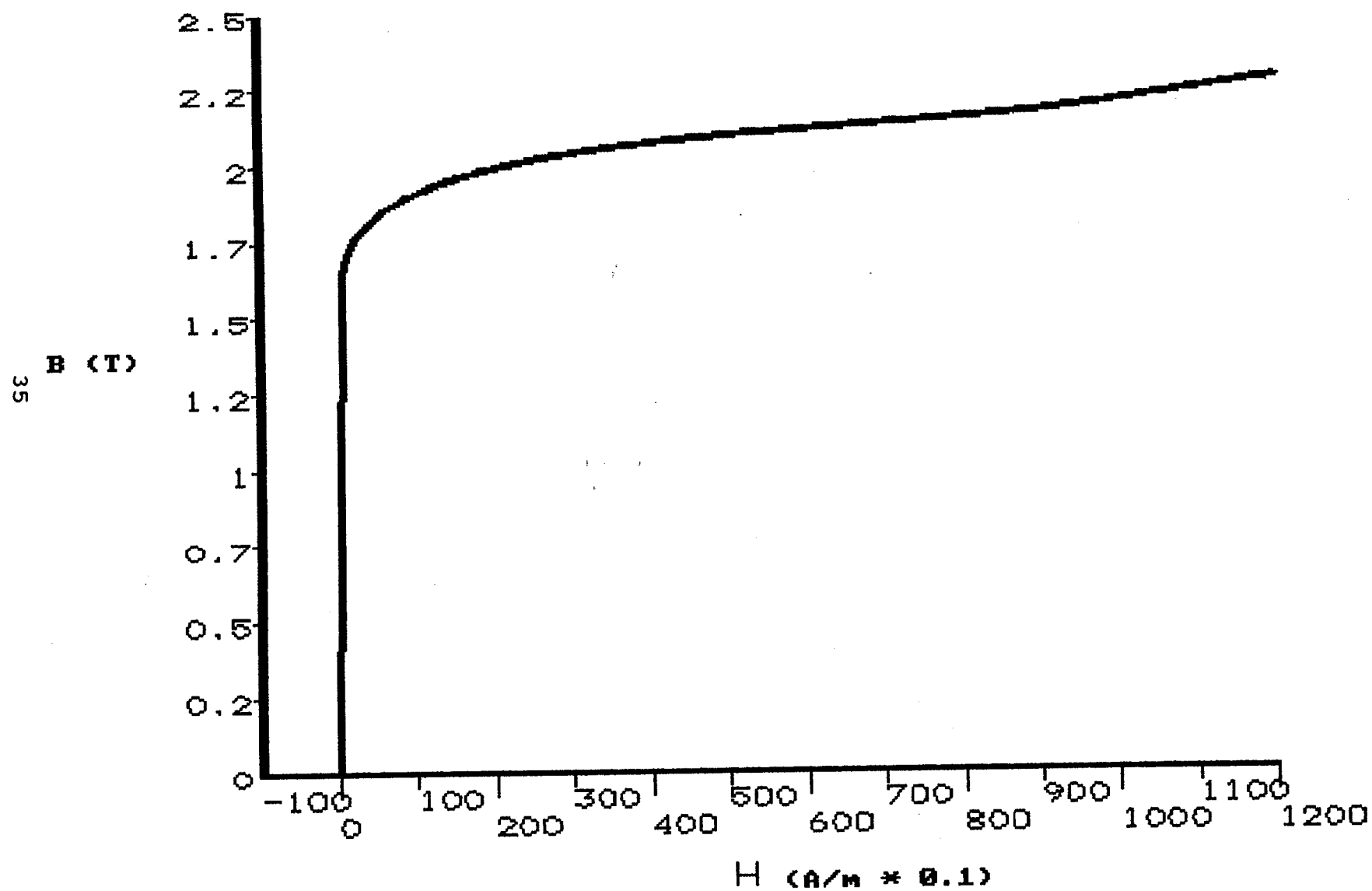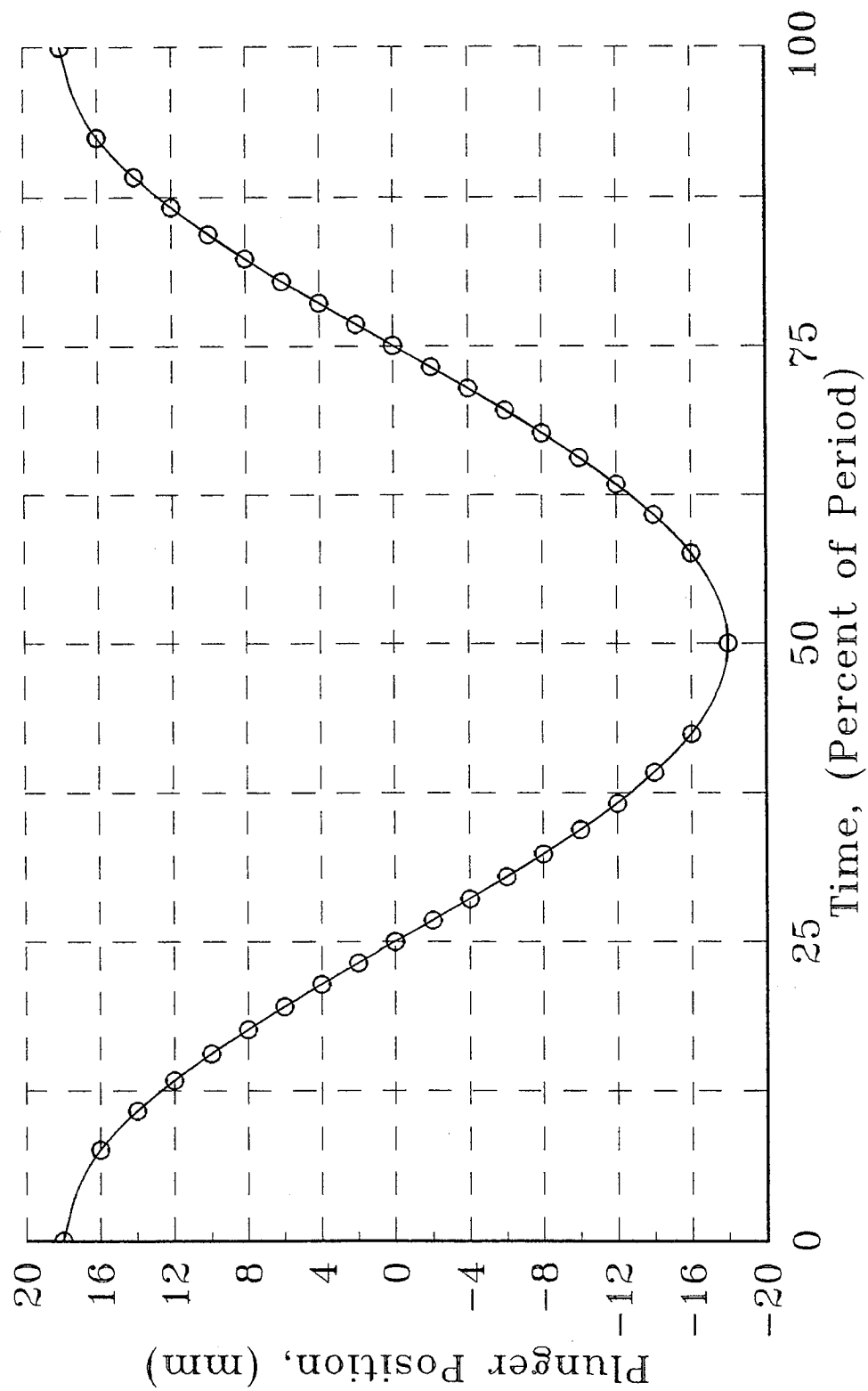Figure 4 – ELEMENT MESH for YOKE and MAGNET SWEPT VOLUME

Figure 5 - Yoke Material (M-19 Si-Fe) Permeance Property Representation

Figure 6
Plunger Position Waveform Discretization

Surface Current Density, Perspective View   2-D FEA Model

Current Direction

"Out-of-Plane Sense"

"Into-Plane Sense"

Nodal Current Loading

z

x   y

Z

R
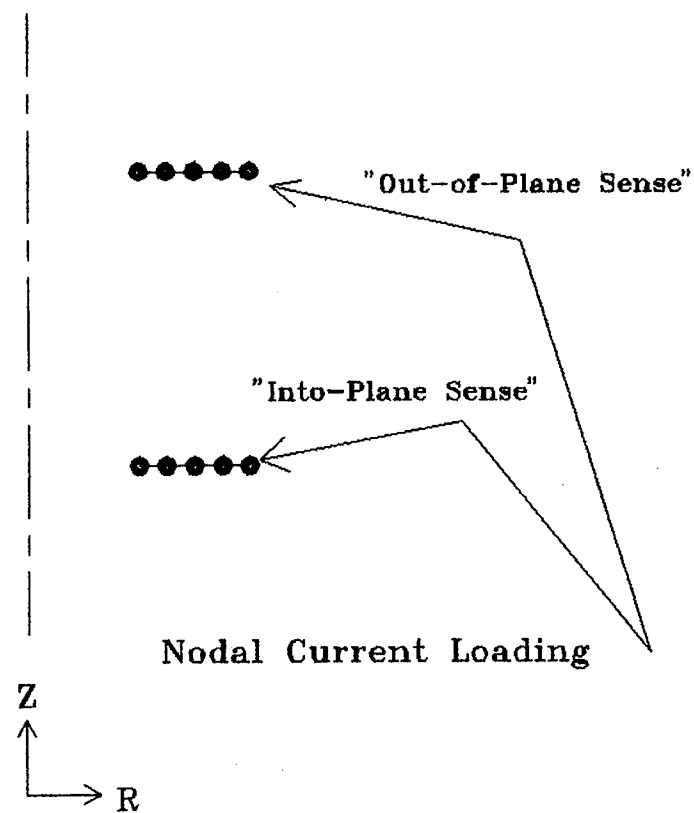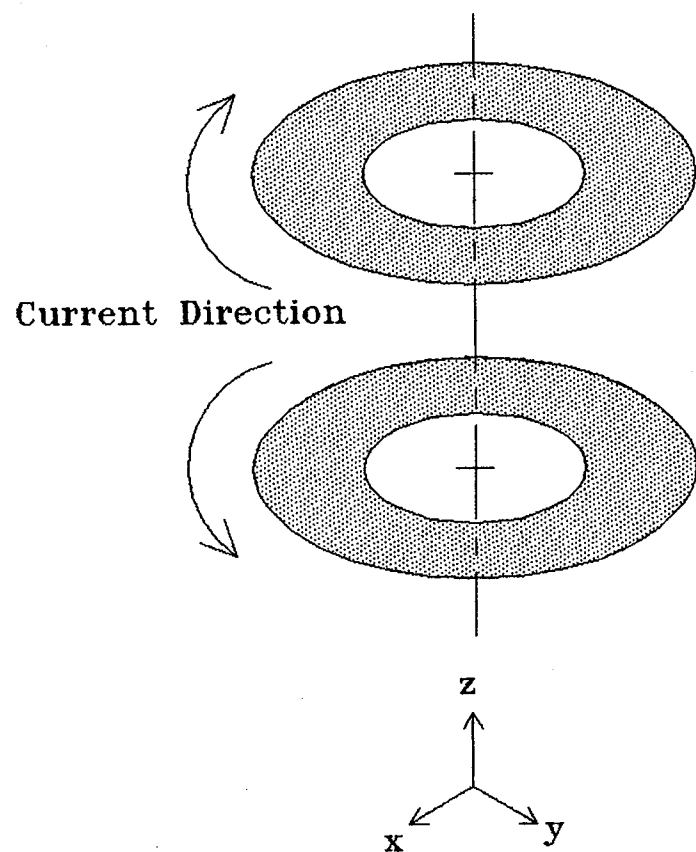
Figure 7 – Amperian Current Equivalent Representation

Magnet Ring, Perspective View   2-D FEA Model

Inside Face
is South Pole

Outside Face
is North Pole

z

x   y

Z

R

Volume
Magnetization Vector
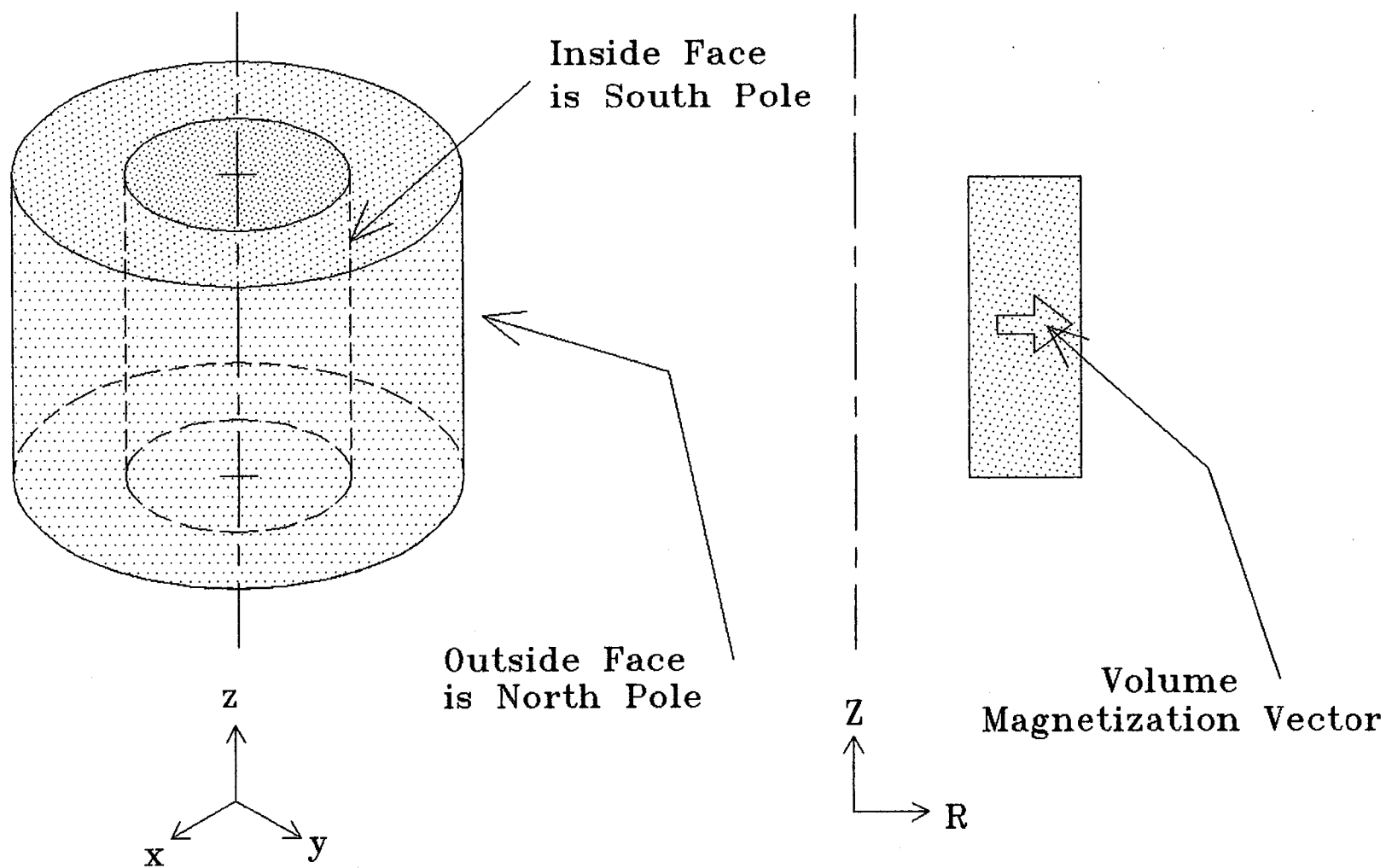
Figure 8 — Direct Magnetized Material Representation

Figure 9 - RELATIVE DIFFERENCE of STATIC FIELD SOLUTIONS (at Xp = 18 mm)

0.054
0.045
0.035
0.025
0.015
0.01
0.005
0.161E-05

39
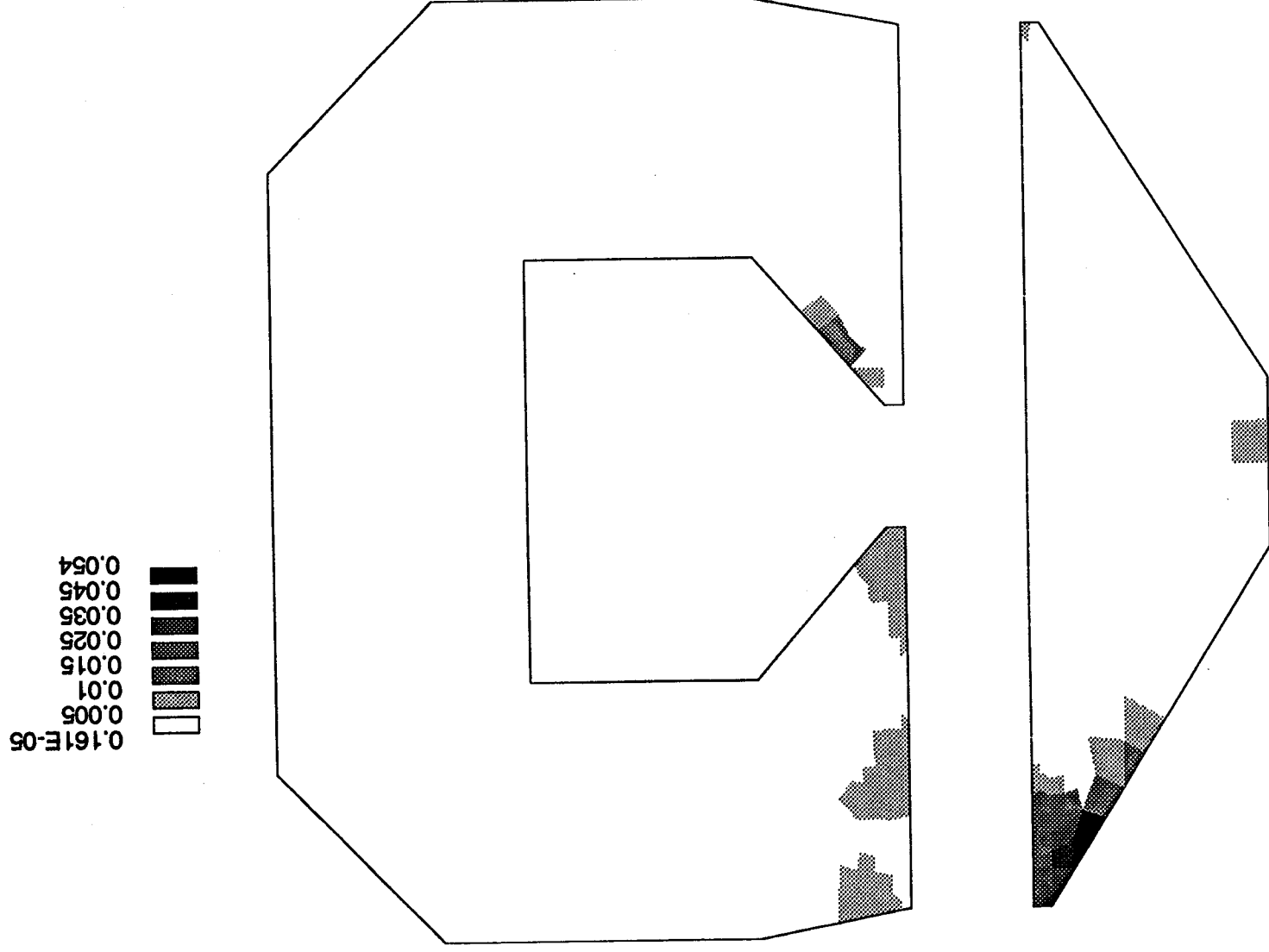
Figure 10 - STATIC FIELD SOLUTION FLUX LINES in YOKE (at Xp = 18 mm)

ANSYS 5.0A 1

40
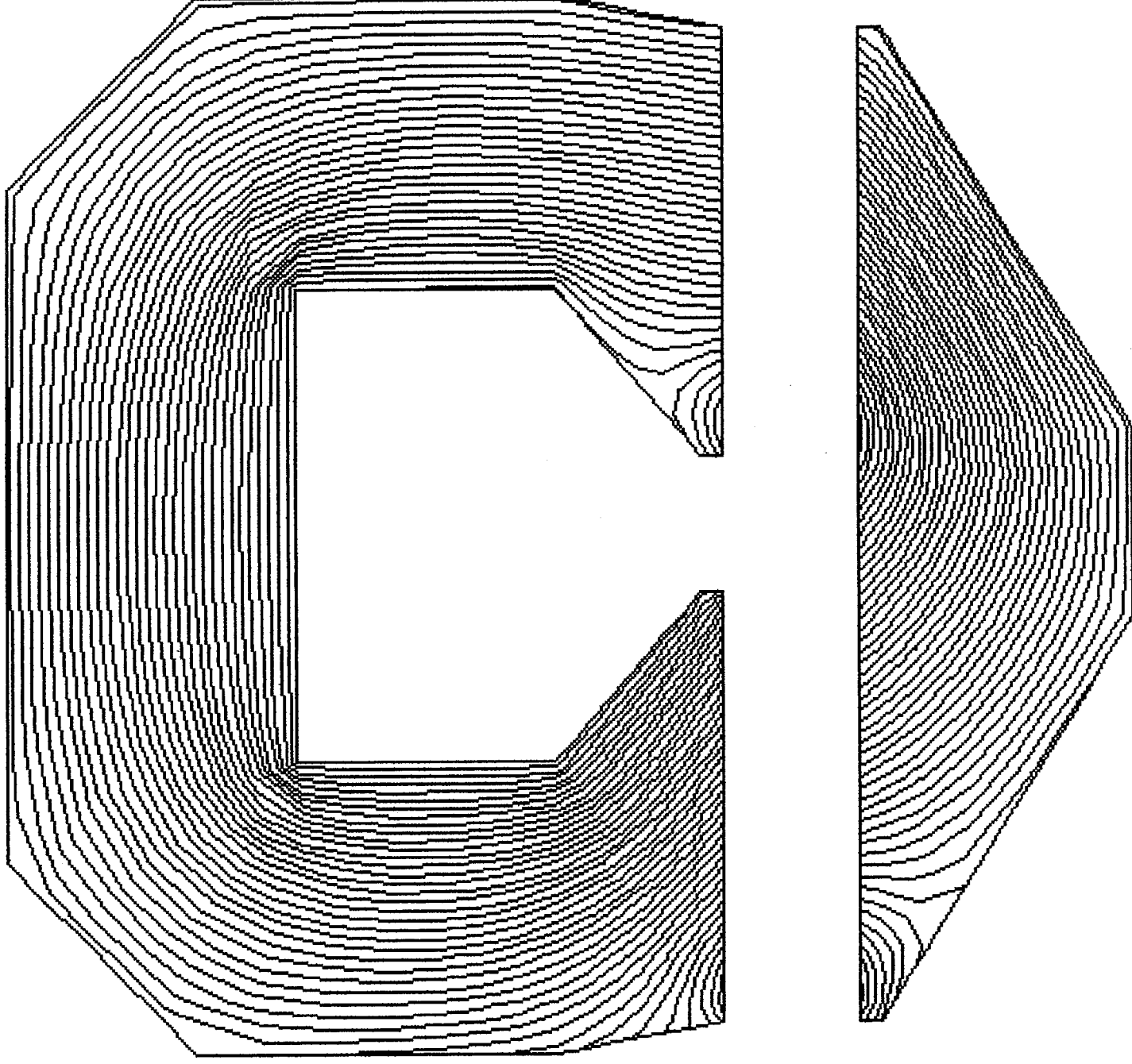
Figure 11
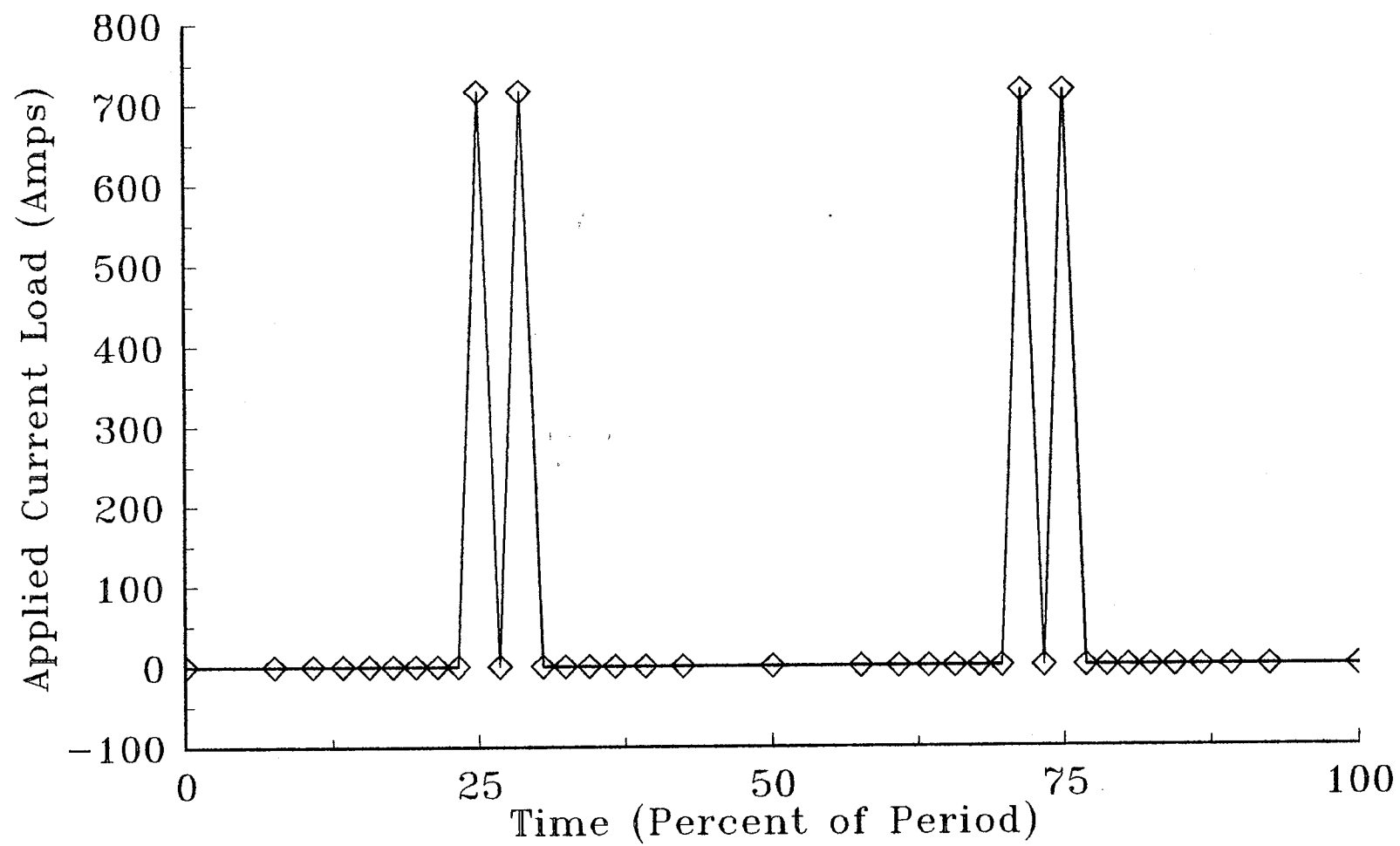Current Load Profile for Typical Node in Swept Volume

41

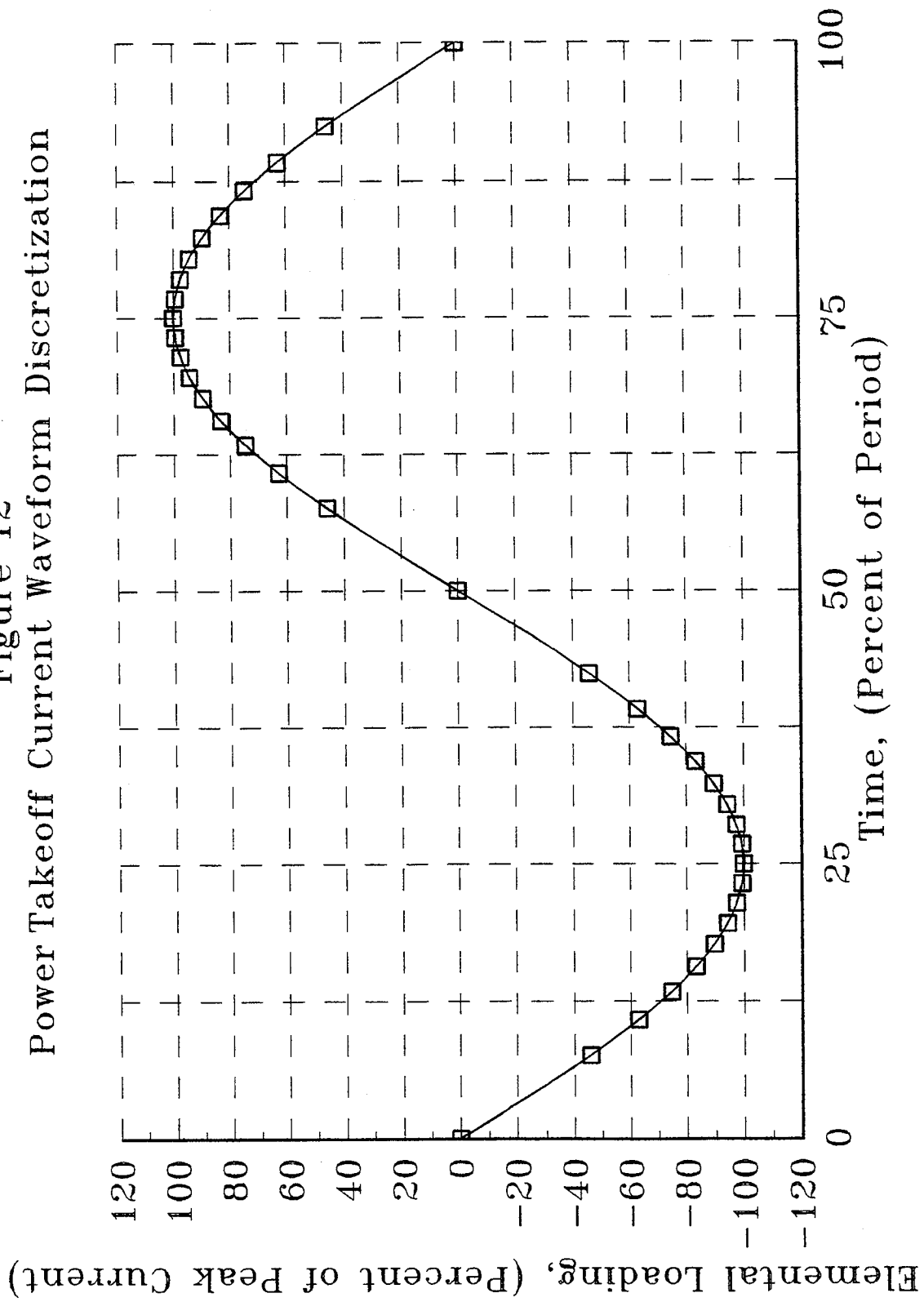Figure 12

Power Takeoff Current Waveform Discretization

FIGURE 13
Percent Change in Instantaneous Power Loss Rate
in Surrounding Structure
Relative to One Cycle Earlier
Volume Integral Over Surrounding Structure.

step	Xp	cycle 2	cycle 3	cycle 4	cycle 5
1	16 mm	+46.309420	+ 0.000410	− 0.000024	0.00
2	14	+24.728591	+ 0.000225	+ 0.000039	0.00
3	12	+16.587144	+ 0.000651	− 0.000491	0.00
4	10	+11.251885	+ 0.000739	− 0.000276	− 0.000001
5	8	+ 9.276285	− 0.000311	+ 0.000549	0.00
6	6	+ 6.827284	+ 0.000192	+ 0.000166	0.00
7	4	+ 5.542882	− 0.000010	+ 0.000160	0.00
8	2	+ 4.283010	+ 0.000208	+ 0.000104	0.00
9	0	+ 3.360418	+ 0.000079	+ 0.000087	0.00
10	− 2	+ 2.550300	+ 0.000233	+ 0.000053	0.00
11	− 4	+14.423661	+ 0.102509	+ 0.001031	+ 0.000016
12	− 6	+ 0.018962	+ 0.001459	+ 0.000017	0.00
13	− 8	− 0.506850	+ 0.000803	+ 0.000011	+ 0.000001
14	−10	− 0.631722	+ 0.000397	+ 0.000007	0.00
15	−12	− 0.626368	+ 0.000173	+ 0.000005	0.00
16	−14	− 0.558872	+ 0.000064	+ 0.000003	0.00
17	−16	− 0.442186	+ 0.000010	+ 0.000002	0.00
18	−18	− 0.221228	+ 0.000016	+ 0.000001	0.00
19	−16	− 0.094493	+ 0.000819	+ 0.000003	0.00
20	−14	− 0.069958	+ 0.001010	+ 0.000014	0.00
21	−12	− 0.050044	+ 0.004392	+ 0.000032	0.00
22	−10	− 0.021621	+ 0.000757	− 0.000024	0.00
23	− 8	− 0.003463	− 0.004494	− 0.000043	0.00
24	− 6	− 0.019593	− 0.003248	− 0.000009	0.00
25	− 4	− 0.026539	− 0.002731	− 0.000143	0.00
26	− 2	− 0.019866	− 0.001699	− 0.000008	0.00
27	0	− 0.014657	− 0.001222	− 0.000006	0.00
28	2	− 0.013029	− 0.000828	− 0.000004	0.00
29	4	− 1.148529	− 0.010400	− 0.000127	− 0.000002
30	6	− 0.021548	− 0.000132	− 0.000002	0.00
31	8	− 0.009301	− 0.000140	− 0.000001	0.00
32	10	− 0.002966	− 0.000125	− 0.000001	0.00
33	12	+ 0.000008	− 0.000102	− 0.000001	0.00
34	14	+ 0.001171	− 0.000081	0.00	0.00
35	16	+ 0.001459	− 0.000066	− 0.000001	0.00
36	18	+ 0.000770	− 0.000040	0.00	0.00

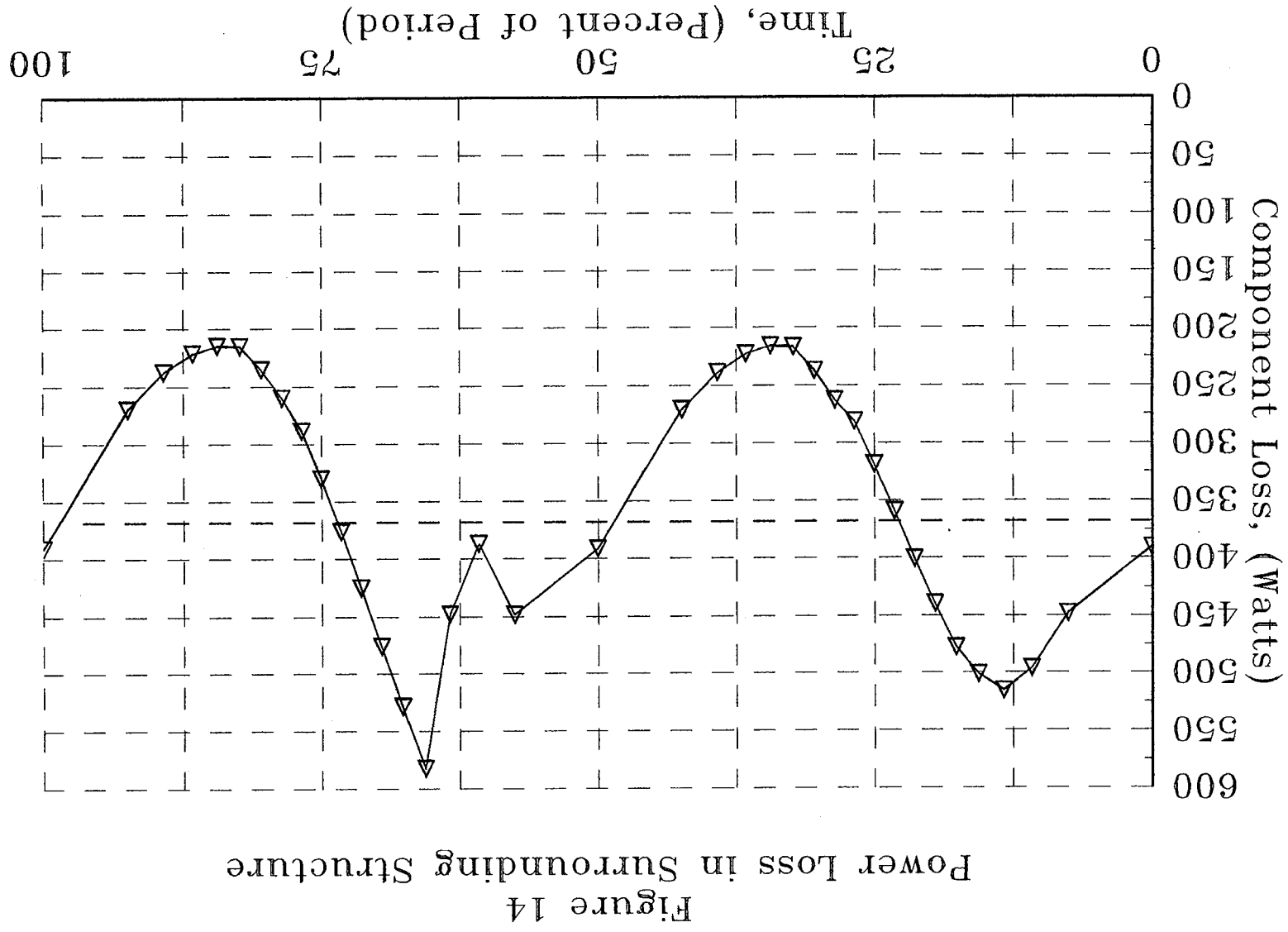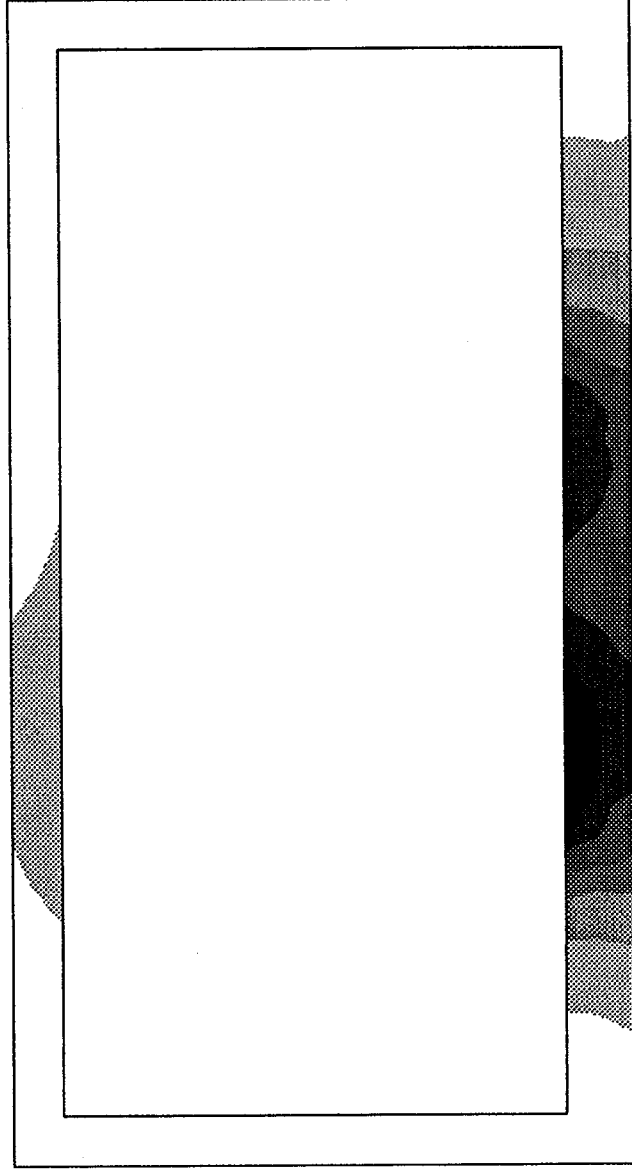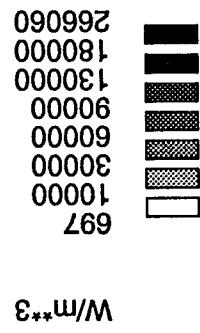| Cycle Averaged Power Loss | | + 5.610373 | + 0.001181 | + 0.000010 | 0.00 |

FIGURE 13

Solution Result Periodicity Verification

Figure 14
Power Loss in Surrounding Structure

Figure 15 - Power Loss Density in Surrounding Structure After Step 5
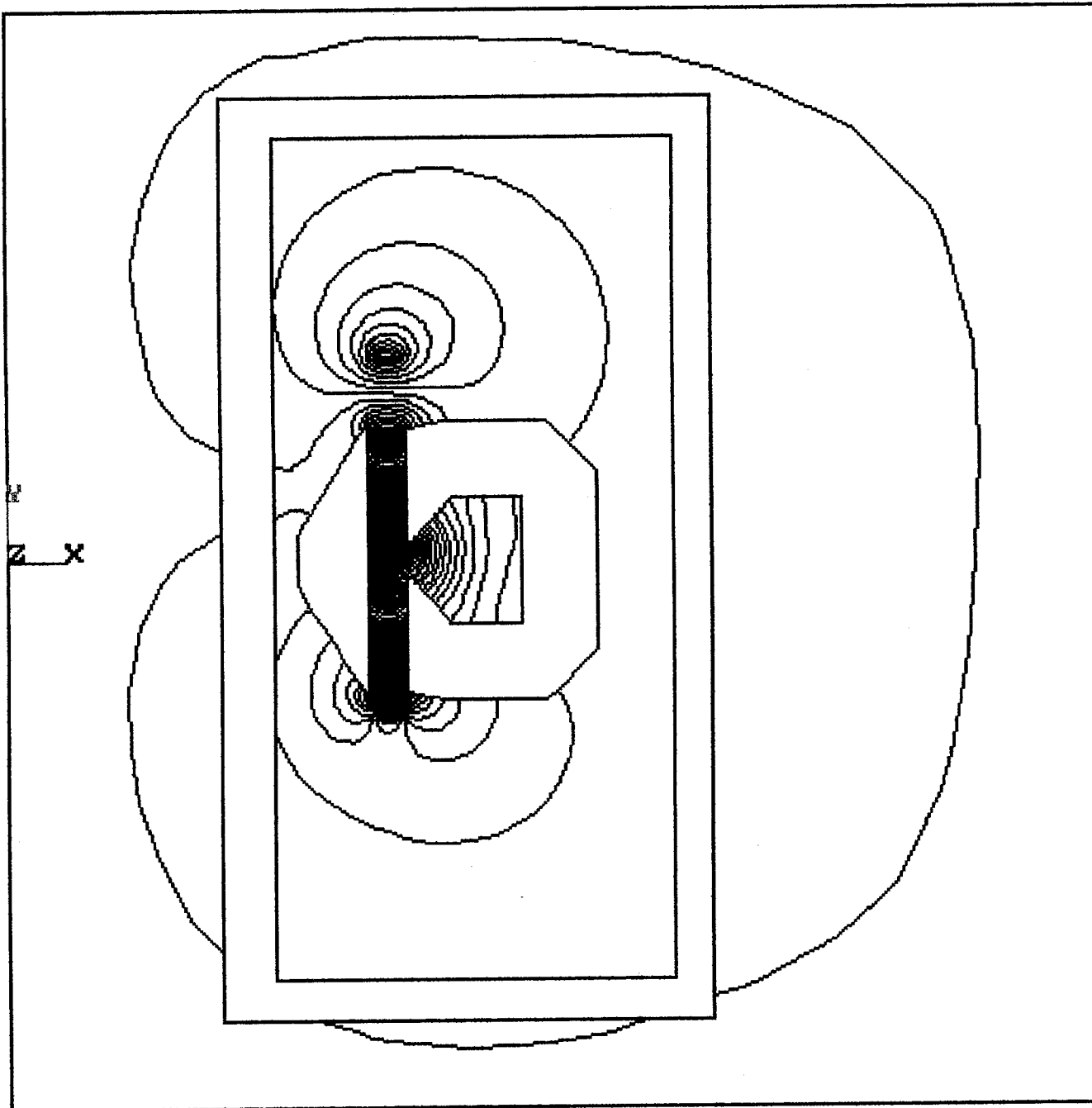
W/m**3

266060
180000
130000
90000
60000
30000
10000
697

Y
X

45

Figure 16 – Fringing Magnetic Flux Lines at End of Step 5
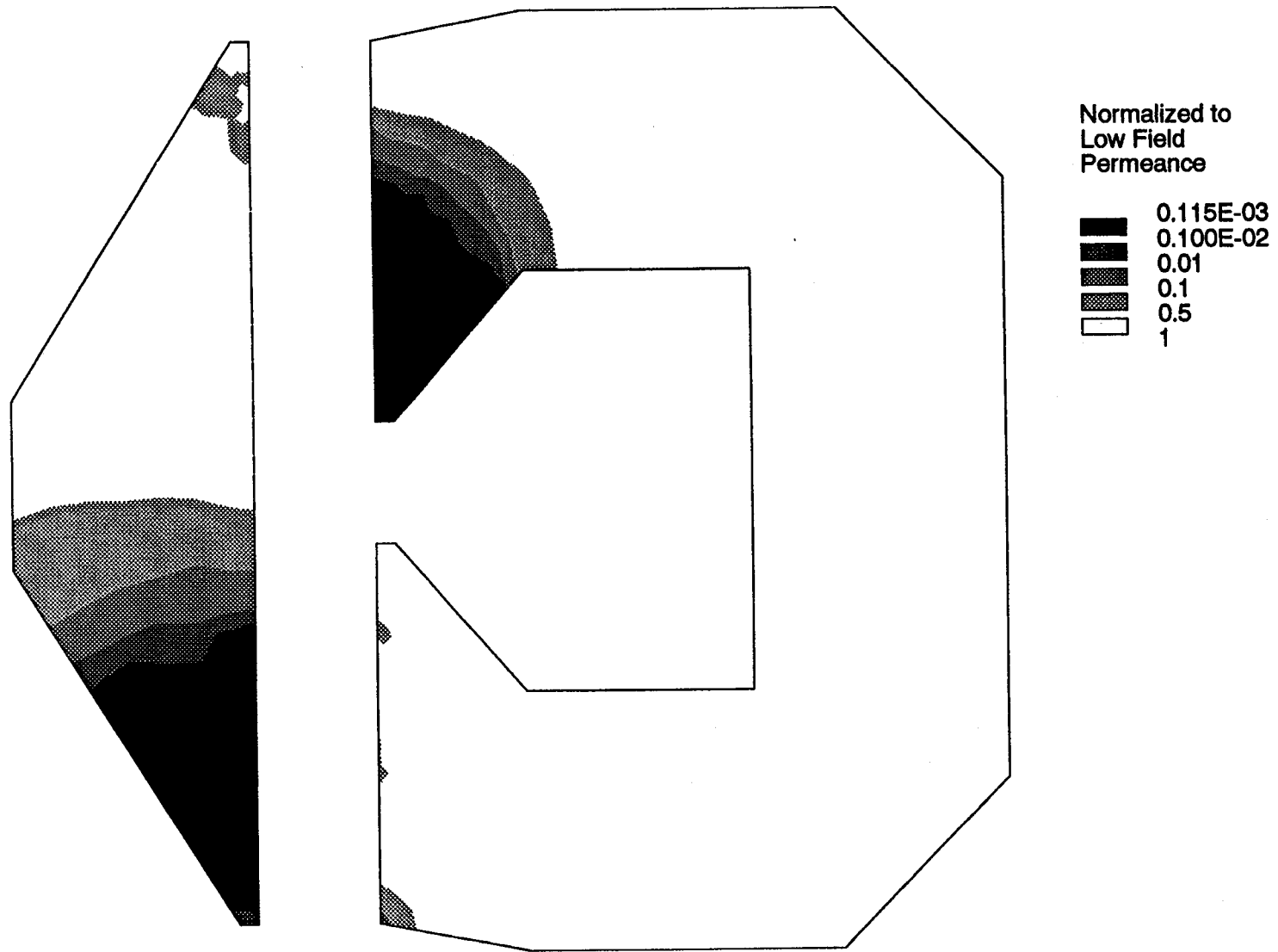
Figure 17 - Normalized Yoke Permeance at End of Step 5

Normalized to
Low Field
Permeance

0.115E-03
0.100E-02
0.01
0.1
0.5
1

47

REPORT DOCUMENTATION PAGE

Public reporting burden for this collection of information is estimated to average 1 hour per response, including the time for reviewing instructions, searching existing data sources, gathering and maintaining the data needed, and completing and reviewing the collection of information. Send comments regarding this burden estimate or any other aspect of this collection of information, including suggestions for reducing this burden, to Washington Headquarters Services, Directorate for Information Operations and Reports, 1215 Jefferson Davis Highway, Suite 1204, Arlington, VA 22202-4302, and to the Office of Management and Budget, Paperwork Reduction Project (0704-0188), Washington, DC 20503.

1. AGENCY USE ONLY (Leave blank)	2. REPORT DATE	3. REPORT TYPE AND DATES COVERED
	December 1995	Final Contractor Report

4. TITLE AND SUBTITLE

Advanced Analysis Technique for the Evaluation of Linear Alternators
and Linear Motors

5. FUNDING NUMBERS

WU–583–02–21
C–NAS3–25827

6. AUTHOR(S)

Jeffrey C. Holliday

7. PERFORMING ORGANIZATION NAME(S) AND ADDRESS(ES)

HOLLIDAYLABS
Guysville, Ohio 45735

8. PERFORMING ORGANIZATION REPORT NUMBER

E–10042

9. SPONSORING/MONITORING AGENCY NAME(S) AND ADDRESS(ES)

National Aeronautics and Space Administration
Lewis Research Center
Cleveland, Ohio 44135–3191

10. SPONSORING/MONITORING AGENCY REPORT NUMBER

NASA CR–198434

11. SUPPLEMENTARY NOTES

12a. DISTRIBUTION/AVAILABILITY STATEMENT

12b. DISTRIBUTION CODE

13. ABSTRACT (Maximum 200 words)

A method for the mathematical analysis of linear alternator and linear motor devices and designs is described, and an example of its use is included. The technique seeks to surpass other methods of analysis by including more rigorous treatment of phenomena normally omitted or coarsely approximated such as eddy braking, non-linear material properties, and power losses generated within structures surrounding the device. The technique is broadly applicable to linear alternators and linear motors involving iron yoke structures and moving permanent magnets. The technique involves the application of Ampérian current equivalents to the modeling of the moving permanent magnet components within a finite element formulation. The resulting steady state and transient mode field solutions can simultaneously account for the moving and static field sources within and around the device.

14. SUBJECT TERMS

Linear alternators; Linear motors; Stirling machines; Electromagnetic analysis

15. NUMBER OF PAGES

49

16. PRICE CODE

A03

17. SECURITY CLASSIFICATION OF REPORT	18. SECURITY CLASSIFICATION OF THIS PAGE	19. SECURITY CLASSIFICATION OF ABSTRACT	20. LIMITATION OF ABSTRACT
Unclassified	Unclassified	Unclassified	

NSN 7540-01-280-5500

Standard Form 298 (Rev. 2-89)
Prescribed by ANSI Std. Z39-18
298-102